Graefe's Arch Clin Exp Ophthalmol
(2006) 244: 58–68

CLINICAL INVESTIGATION

DOI 10.1007/s00417-005-0029-0

Akiyasu Kanamori
Azusa Nagai-Kusuhara
Michael F. T. Escaño
Hidetaka Maeda
Makoto Nakamura
Akira Negi

Comparison of confocal scanning laser ophthalmoscopy, scanning laser polarimetry and optical coherence tomography to discriminate ocular hypertension and glaucoma at an early stage

Received: 17 January 2005
Revised: 6 April 2005
Accepted: 4 May 2005
Published online: 26 July 2005

A. Kanamori (✉) · A. Nagai-Kusuhara · M. F. T. Escaño · H. Maeda · M. Nakamura · A. Negi
Division of Ophthalmology, Department of Organ Therapeutics, Kobe University Graduate School of Medicine,
7-5-2 Kusunoki-cho, Chuo-ku,
Kobe, 650-0017, Japan
e-mail: kanaaki@med.kobe-u.ac.jp
Tel.: +81-78-3826048
Fax: +81-78-3826059

Abstract *Background:* The aim was to compare the ability of confocal scanning laser ophthalmoscopy (CSLO), scanning laser polarimetry (SLP), and optical coherence tomography (OCT) to discriminate eyes with ocular hypertension (OHT), glaucoma-suspect eyes (GS) or early glaucomatous eyes (EG) from normal eyes. *Methods:* Ocular hypertension, GS, and EG were defined as normal disc with intraocular pressure >21 mmHg, glaucomatous disc without visual field loss, and glaucomatous disc accompanying the early glaucomatous visual filed loss respectively. Ninety-three normal eyes, 26 OHT, 55 GS, and 67 EG were enrolled. Optic disc configuration was analyzed by CSLO (version 3.04), whereas retinal nerve fiber layer thickness was analyzed by SLP (GDx-VCC; version 5.3.2) and OCT-1 (version A6X1) in each individual. The measurements were compared in the four groups of patients. Receiver operating characteristic curve (ROC) and area under the curve (AUC) discriminating OHT, GS or EG from normal eyes were compared for the three instruments. *Results:* Most parameters in GS and EG eyes showed significant differences compared with normal eyes. However, there were few significant differences between normal and OHT eyes. No significant differences were observed in AUCs between SLP and OCT. In EG eyes, the greatest AUC parameter in OCT (inferior—120; 0.932) had a higher AUC than that in CSLO (vertical cup/disc ratio; 0.845; P=0.017). In GS, the greatest AUC parameter in OCT (average retinal nerve fiber layer [RNFL] thickness; 0.869; P=0.002) and SLP (nerve fiber indicator [NFI]; 0.875; P=0.002) had higher AUC than that in CSLO (vertical cup/disc ratio; 0.720). *Conclusions:* Three instruments were useful in identifying GS and EG eyes. For glaucomatous eyes with or without early visual field defects, SLP and OCT performed similarly or had better discriminating abilities compared with CSLO.

Keywords Glaucoma · Optical coherence tomography · Scanning laser polarimetry · Confocal scanning laser ophthalmoscopy · Early stage

Introduction

Glaucoma is an optic neuropathy characterized by progressive injury of the optic nerve and retinal nerve fiber layer (RNFL) [26, 30]. Although visual field testing has a high specificity for detection of glaucoma, the loss of optic nerve fibers usually precedes the development of reproducible glaucomatous visual field defects [21, 30]. Therefore, detection of early glaucoma using ocular imaging technology has recently gained much clinical interest.

Various ocular imaging instruments, such as confocal scanning laser ophthalmoscopy (CSLO), scanning laser

polarimetry (SLP), and optical coherence tomography (OCT), have recently become available. CSLO is able to analyze a three-dimensional optic nerve head configuration [3]. SLP and OCT can measure RNFL thickness around the optic disc [9, 24]. Many investigators demonstrated the advantages and disadvantages of these instruments in detecting glaucomatous damage. However, comparison across studies is difficult due to differences in study design and characteristics of the patient population. In addition to individual variability of the optic disc and RNFL thickness [19, 22], the aging effect including axonal loss limits the ability to accurately detect glaucoma [12, 13, 19]. Hence, it is of importance to use similar population characteristics when comparing the performance of these instruments. In addition, since these instruments are relatively rapidly updated for accuracy, serial assessments of parameters tested with these instruments are needed to validate their clinical value.

This study was designed to compare within a similar population the abilities of CSLO, SLP, and OCT to discriminate early glaucomatous eyes from normal eyes. In addition, we evaluated whether these instruments could detect very early structural damage in glaucoma-suspect eyes or eyes with ocular hypertensive without abnormalities in the achromatic visual field.

Materials and methods

This study was a retrospective, nonrandomized study, which was performed at the Department of Ophthalmology of the Kobe University Hospital between April 2003 and November 2003. This non-invasive study was conducted in accordance with the ethical standards stated in the 1964 Declaration of Helsinki. This study was approved by the Ethical Committee of Kobe University Graduate School of Medicine and informed consent was obtained from all participants.

All subjects had a negative history for diabetes mellitus and underwent a full ophthalmic examination. All eyes had a best-corrected visual acuity of at least 20/40 with a refractive error of <4 dioptric astigmatism without retinal disease and significant vitreous opacity. Intraocular pressure (IOP) was measured by Goldmann applanation tonometry. Stereoview examination of the optic disc configuration was performed with slitlamp biomicroscopy and contact or noncontact pre-placed lens. The glaucomatous optic disc change was determined when three glaucoma experts (AK, NM, and AN) agreed the judgement. Glaucomatous optic neuropathy was defined as vertical cup-disc asymmetry between fellow eyes of 0.2 or more and neuroretinal rim damages such as excavation, rim thinning, and notches with or without peripapillary hemorrhages or RNFL defects.

Achromatic automated perimetry was performed with the Humphrey Field Analyzer (Humphrey-Zeiss Instruments, Dublin, CA, USA) using central SITA-standard program 30-2. Visual field reliability criteria included fixation losses and false-positive and false-negative rates of less than 25%. Glaucomatous eyes were defined as glaucomatous optic neuropathy plus associated visual field loss. The evaluation of glaucomatous visual field defects was based on liberal criteria (two or more contiguous points with a pattern deviation sensitivity loss of $P<0.01$, or three or more contiguous points with sensitivity loss of $P<0.05$, in the superior or inferior arcuate areas, or a 10-dB difference across the nasal horizontal midline at two or more adjacent locations and an abnormal result in the glaucoma hemifield test) [2].

When glaucomatous optic neuropathy was judged, the experts were masked to the results of the three instruments. Reproducible visual field, CSLO, SLP, and OCT examinations in the same individuals were performed within a maximum period of 6 months.

Subjects

Patients who underwent any ocular surgeries were excluded from this study.

Normal subjects with a negative family history of glaucoma, normal optic disc appearance, and normal intraocular pressure were used as controls, from each of whom one eye was randomly selected.

Eyes with ocular hypertension (OHT) were defined as eyes with an IOP reading of >21 mmHg on at least two separate occasions in an individual meeting all of the normal visual field and normal optic disc criteria. Glaucoma-suspect eyes (GS) was defined as eyes having the glaucomatous optic neuropathy mentioned above without any corresponding visual field defect. Early glaucomatous eyes (EG) had glaucomatous visual field defects defined as mean deviation >−6 dB by the Humphrey Field Analyzer.

Confocal scanning laser ophthalmoscope

Confocal scanning was performed in a standard fashion using the Heidelberg Retina Tomograph (HRT, version 3.04, Heidelberg Engineering, Heidelberg, Germany). HRT-1 hardware with HRT-2 software was used in this study. Three 20° topographic images were obtained from each eye without pupillary dilation. A composite image created from these three images was used for analyses. The disc margin contour line to determine the disc area was drawn by one of the authors (ANK) at the inner edge of the scleral ring during comparison with optic disc photographs. An image was considered of good quality if the mean SD of height measurements was less than 40 μm. Disc area, rim area, cup/disc ratio, cup volume, rim volume, measurement of cup shape, mean RNFL thickness, horizontal cup/disk ratio, vertical cup/disk ratio, the F S Mikelberg (FSM) discriminant function value provided by Iester et al [11] and the R

Bathija (RB) discriminant function value provided by Burk (Heidelberg Retina Tomograph 2; Operating Instructions, Dossenheim, Germany) were all evaluated from global data. The sectors used in this study were classified into the following: superior = 315°–345°; nasal = 45°–135°; inferior = 135°–225°; and temporal = 225°–315°.

Scanning laser polarimetry

GDx with variable corneal compensation (GDx-VCC, Laser Diagnostic Technologies, Inc., San Diego, CA, USA) was used as SLP of a 780-nm diode laser. In GDx-VCC, the compensating retarders are adjusted to minimize the effects of individual anterior segment birefringence, such as from the cornea and lens [31]. With version 5.3.2 software installed in our GDx-VCC, one macular polarimetry image was taken to measure the anterior segment birefringence from each eye without pupillary dilation. Then, parapapillary RNFL thickness measurements compensated by the earlier macular image were performed by one author (AK). Concentric circle measurements were centered on the optic disc with an outer and inner radius of 1.628 mm and 1.256 mm respectively. Images were accepted only if the quality score fell within 8–10 and an "OK" sign was displayed in the embedded image checking system.

Fifteen parameters were automatically evaluated. The sectors defined by the software were: superior = 295°–355°; nasal = 55–125°; inferior = 125°–245°; and temporal = 245°–295°.

Optical coherence tomography

The OCT-1 (Humphrey Zeiss Instruments, Dublin, CA, USA) was used. Three circular scans, each 3.4 mm in diameter, centered on the optic disc, were obtained from each eye after pupillary dilation [7] by one of the authors (AK). The RNFL thickness was calculated from the three scans using the standard RNFL thickness program (version A6X1). Eyes with incomplete or distorted images, or with images having less than 45 dB signal–noise ratio were excluded.

Three different parameters were evaluated. First was the average RNFL thickness of the entire circumference of the optic disc. The second parameter was the four quadrant thickness. The third parameter was segmental thickness per 30-degree radian. Furthermore, to approximate the sector in the SLP measurements, the mean thickness from the segmental thickness parameters was calculated based on the following: superior 120 = 295°–355°; nasal 70 = 55–125°; inferior 120 = 125°–245°; and temporal 50 = 245°–295°.

Statistical analyses

All data were exported into a personal computer. Bilateral eyes of 21 subjects with OHT (n=7), GS (n=10), and EG (n=4) were mixed for the following analyses in this study. Otherwise, left eye data were converted into the right eye format. All statistical analyses were performed using Stat View 5.0 (SAS Institute, Cary, NC, USA) and Med Calc (Frank Schoonjans, Mariakerke, Belgium).

Multiple comparisons between groups were conducted in all parameters using analysis of variance. Paired comparisons for all significant main effects were conducted using the Tukey–Kramer post-hoc test. Data were reported as mean ± standard deviation (SD). A P value of less than 0.05 was accepted as statistically significant.

The receiver operating characteristic (ROC) curve was used to describe the ability of each parameter to discriminate OHT, GS, and EG from normal eyes. A perfect test would have an area under the curve (AUC) of 1, whereas a test without diagnostic value would have an AUC of 0.5 [1]. The method of Hanley and McNeil [6] was used to compare the AUCs of the different parameters. Sensitivity and specificity for detection of glaucomatous eyes were determined by obtaining the highest sensitivity values with target specificity set at ≥95% and ≥85%.

Results

Eleven, 10, and 11 eyes were excluded because of poor image in normal eyes, GS and EG respectively. Eventually, 93 normal eyes, 26 eyes of 19 patients with OHT, 55 eyes of 45 GS patients, and 67 eyes of 63 EG patients were

Table 1 Patient demographics

	Normal (n=93)	OHT (n=26)	GS (n=55)	EG (n=67)	P value
Age (years), mean ± SD	45.0±15.5	46.4±11.4	48.5±12.3	48.9±12.6	0.244*
Gender					
Male	53	14	22	30	0.109†
Female	40	12	33	37	
Refraction (diopters), mean ± SD	−2.38±2.96	−1.25±2.54	−2.16±3.13	−2.41±3.50	0.352
MD in HFA (dB), mean ± SD	−0.48±0.92	−0.63±1.11	−1.14±1.41	−3.55±1.76	<0.001*‡
PSD in HFA (dB), mean ± SD	1.00±0.63	1.24±0.88	1.46±0.98	6.26±10.82	<0.001*‡

OHT ocular hypertension, *GS* glaucoma-suspect, *EG* early glaucoma, *MD* mean deviation, *HFA* Humphrey field analyzer, *PSD* pattern standard deviation
*Analysis of variance
†Chi-squared
‡EG significantly differed from other group (Tukey-Kramer test)

Table 2 Comparison of confocal scanning laser ophthalmoscope (CSLO) measurements in control, OHT, GS, and EG eyes

Parameter	Control	OHT	GS	EG	*P* value
Global					
Disc area	2.45±0.693	2.61±0.602	2.63±0.658	2.54±0.551	0.396
Rim area	1.70±0.436	1.76±0.244	1.52±0.357	1.30±0.305	<0.001*†§¶
Cup/disc area ratio	0.286±0.143	0.303±0.130	0.404±0.150	0.832±0.036	<0.001*†‡§¶
Cup volume	0.193±0.192	0.243±0.231	0.306±0.227	0.339±0.219	<0.001*†§
Rim volume	0.472±0.204	0.493±0.164	0.374±0.166	0.299±0.131	<0.001*†‡§
Cup shape measure	−0.163±0.076	−0148±0.063	−0.102±0.071	−0.069±0.075	<0.001*†§
Mean RNFL thickness	0.256±0.091	0.254±0.087	0.221±0.064	0.198±0.068	<0.001†§
Horizontal cup/disc ratio	0.550±0.195	0.535±0.169	0.628±0.162	0.719±0.134	<0.001†§
Vertical cup/disc ratio	0.430±0200	0.462±0.204	0.569±0.0191	0.651±0144	<0.001*†§
FSM	1.673±2.155	1.834±1.512	0.391±1.723	0.640±1.552	<0.001*†‡§¶
RB	1.130±1.02	1.134±1.03	0.459±1.10	0.107±0.692	<0.001*†‡
Superior					
Disc area	0.320±0.087	0.346±0.079	0.347±0.086	0.337±0.075	0.159
Rim area	0.236±0.061	0.240±0.031	0.208±0.054	0.185±0.047	<0.001*†§
Cup/disc area ratio	0.244±0.152	0.266±0.160	0.378±0.170	0.435±0.154	<0.001*†‡§
Cup volume	0.027±0.030	0.036±0.041	0.046±0.036	0.048±0.035	<0.001*†
Rim volume	0.077±0.034	0.078±0.024	0.060±0.028	0.050±0.023	<0.001*†‡§
Cup shape measure	0.112±0.122	0.073±0.139	0.033±0.137	0.007±0.134	<0.001*†
Mean RNFL thickness	0.339±0.123	0.351±0.108	0.294±0.112	0.272±0.089	<0.001†§
Temporal					
Disc area	0.594±0.181	0.598±0.149	0.622±0.164	0.594±0.132	0.743
Rim area	0.291±0.119	0.277±0.085	0.228±0.080	0.199±0.061	<0.001†§
Cup/disc area ratio	0.493±0.180	0.522±0.120	0.613±0.172	0.652±0.120	<0.001*†§
Cup volume	0.071±0.061	0.091±0.067	0.091±0.061	0.103±0.067	0.015†
Rim volume	0.034±0.020	0.035±0.018	0.021±0.011	0.018±0.010	<0.001*†‡§
Cup shape measure	−0.080±0.095	−0.066±0.068	−0.041±0.089	−0.010±0.080	<0.001*†§
Mean RNFL thickness	0.089±0.025	0.086±0.015	0.080±0.021	0.074±0.022	<0.001†
Inferior					
Disc area	0.327±0.087	0.346±0.077	0.345±0.085	0.337±0.075	0.121
Rim area	0.232±0.059	0.241±0.047	0.211±0.062	0.177±0.054	<0.001†§
Cup/disc area ratio	0.247±0.046	0.275±0.156	0.366±0.179	0.462±0.151	<0.001*†§¶
Cup volume	0.022±0.022	0.027±0.030	0.035±0.031	0.042±0.027	<0.001*†
Rim volume	0.067±0.030	0.072±0.031	0.054±0.030	0.040±0.022	<0.001*†‡§
Cup shape measure	−0.122±0.108	−0.096±0.080	−0.026±0.125	−0.009±0.109	<0.001*†§
Mean RNFL thickness	0.293±0.106	0.302±0.129	0.246±0.116	0.210±0.088	<0.001†§
Nasal					
Disc area	0.596±0.179	0.605±0.150	0.627±0.169	0.599±0.134	0.716
Rim area	0.473±0.145	0.494±0.083	0.450±0.134	0.380±0.119	<0.001†§¶
Cup/disc area ratio	0.181±0.166	0.155±0.153	0.263±0.181	0.355±0.185	<0.001†§¶
Cup volume	0.029±0.044	0.028±0.040	0.053±0.059	0.099±0.059	0.003†
Rim volume	0.149±0.077	0.149±0.067	0.126±0.058	0.040±0.022	<0.001†§
Cup shape measure	−0.173±0.142	−0.203±0.123	−0.120±0.147	−0.079±0.158	<0.001†
Mean RNFL thickness	0.299±0.132	0.284±0.132	0.264±0.126	0.235±0.127	0.028†

FSM F S Mikelberg discriminant function, *RB* R Bathija discriminant function
*Control is significantly different from GS
†Control is significantly different from EG
‡OHT is significantly different from GS
§OHT is significantly different from EG
¶EG is significantly different from GS

Table 3 Area under the curve for CSLO

Parameter	OHT	GS	EG
Global			
Disc area	0.550±0.069	0.566±0.051	0.549±0.048
Rim area	0.557±0.068	0.610±0.049	0.753±0.039
Cup/disc area ratio	0.519±0.069	0.712±0.047	0.832±0.036
Cup volume	0.568±0.068	0.654±0.050	0.716±0.044
Rim volume	0.553±0.067	0.640±0.047	0.753±0.039
Cup shape measure	0.553±0.068	0.722±0.047	0.809±0.037
Mean RNFL thickness	0.523±0.068	0.640±0.047	0.697±0.042
Horizontal cup/disk ration	0.540±0.068	0.623±0.050	0.764±0.041
Vertical cup/disk ratio	0.552±0.069	0.720±0.047	0.845±0.034
FSM	0.559±0.068	0.658±0.047	0.815±0.034
RB	0.501±0.069	0.688±0.045	0.791±0.036
Superior			
Disc area	0.588±0.069	0.599±0.051	0.581±0.048
Rim area	0.564±0.068	0.612±0.049	0.770±0.040
Cup/disc area ratio	0.545±0.069	0.718±0.046	0.812±0.037
Cup volume	0.589±0.068	0.689±0.048	0.733±0.043
Rim volume	0.568±0.068	0.648±0.047	0.721±0.041
Cup shape measure	0.582±0.069	0.669±0.049	0.757±0.041
Mean RNFL thickness	0.510±0.068	0.630±0.048	0.671±0.043
Temporal			
Disc area	0.507±0.068	0.549±0.051	0.501±0.048
Rim area	0.501±0.068	0.650±0.047	0.742±0.040
Cup/disc area ratio	0.543±0.069	0.719±0.047	0.769±0.040
Cup volume	0.607±0.068	0.608±0.051	0.659±0.046
Rim volume	0.502±0.069	0.709±0.044	0.759±0.038
Cup shape measure	0.601±0.069	0.645±0.050	0.748±0.042
Mean RNFL thickness	0.563±0.069	0.649±0.047	0.711±0.041
Inferior			
Disc area	0.582±0.068	0.598±0.051	0.588±0.047
Rim area	0.584±0.069	0.585±0.049	0.797±0.038
Cup/disc area ratio	0.552±0.069	0.701±0.048	0.842±0.035
Cup volume	0.577±0.069	0.642±0.050	0.753±0.041
Rim volume	0.575±0.069	0.639±0.047	0.766±0.038
Cup shape measure	0.568±0.069	0.642±0.050	0.774±0.040
Mean RNFL thickness	0.523±0.069	0.654±0.047	0.726±0.041
Nasal			
Disc area	0.517±0.069	0.545±0.051	0.521±0.048
Rim area	0.560±0.069	0.554±0.050	0.685±0.043
Cup/disc area ratio	0.542±0.068	0.631±0.050	0.756±0.041
Cup volume	0.548±0.067	0.627±0.050	0.709±0.044
Rim volume	0.503±0.069	0.590±0.049	0.702±0.042
Cup shape measure	0.562±0.067	0.662±0.046	0.662±0.046
Mean RNFL thickness	0.556±0.067	0.587±0.049	0.648±0.044

Table 4 Comparison of scanning laser polarimetry (SLP) parameters in control, OHT, GS and EG eyes

Parameter (mean±SD)	Control	OHT	GS	EG	*P* value
TSNIT average	57.8±5.07	55.8±6.95	49.4±6.37	46.7±7.29	<0.001*†
Superior average	70.3±7.65	68.9±7.35	60.1±8.28	56.4±10.5	<0.001*†
Inferior average	70.0±9.49	65.9±11.0	56.8±9.66	51.6±11.2	<0.001*†‡
TSNIT SD	25.4±4.55	23.5±4.26	19.1±3.84	18.0±4.78	<0.001*†
NFI	16.8±7.84	18.6±7.45	32.3±12.0	43.9±19.9	<0.001*†‡
Symmetry	0.97±0.16	1.01±0.17	1.02±0.19	1.03±0.21	0.203
Superior ratio	3.14±1.14	3.10±1.10	2.46±0.61	2.35±0.87	<0.001*†
Inferior ratio	3.27±1.17	3.31±1.14	2.46±0.68	2.30±0.85	<0.001*†
Superior/nasal	3.18±0.81	2.90±0.66	2.69±0.75	2.44±0.57	<0.001*§
Maximum modulation	2.92±0.99	2.70±1.01	2.06±0.74	1.87±0.71	<0.001*†
Superior maximum	84.4±11.4	81.7±12.7	71.2±12.7	67.0±13.0	<0.001*†
Inferior maximum	88.1±11.6	81.5±14.5	70.8±11.7	66.0±13.3	<0.001*†
Ellipse modulation	4.19±1.33	3.81±1.20	3.14±1.03	3.10±0.99	<0.001*†
Normalized superior area	0.157±0.027	0.144±0.024	0.115±0.025	0.104±0.033	<0.001*†
Normalized Inferior area	0.157±0.028	0.142±0.037	0.114±0.031	0.100±0.035	<0.001*†

NFI nerve fiber indicator, *TSNIT* temporal, superior, nasal, inferior, temporal
*Control is significantly different from GS and EG
†OHT is significantly different from GS and EG
‡EG is significantly different from GS
§OHT is significantly different from EG

enrolled in this study. Table 1 summarizes the patient demographics. With regard to age, gender, and refraction, there were no significant differences in the four groups.

Comparison of the measurements and AUCs in the subject groups

Table 2 summarizes the mean ± SD in all parameters measured by CSLO. There were no significant differences in the disc area in all sectors of all groups. Most parameters in the GS and EG group were significantly different from the normal group. There was no significant difference in any of the parameters between the control and OHT groups. AUCs from CSLO is shown in Table 3. CSLO parameters with the greatest AUC in the EG, GS, and OHT eyes were vertical cup/disc ratio, global cup shape measure, and temporal cup volume respectively.

Table 4 summarizes the mean ± SD in all parameters measured by SLP. Most parameters for GS and EG were significantly different from the control and OHT. There were no parameters showing a significant difference be-

Table 5 Area under the curve of SLP parameters

Parameter (mean ± SD)	OHT	GS	EG
TSNIT average	0.644±0.059	0.850±0.031	0.895±0.025
Superior average	0.543±0.065	0.814±0.034	0.869±0.028
Inferior average	0.642±0.059	0.845±0.031	0.905±0.024
TSNIT SD	0.624±0.060	0.857±0.030	0.865±0.028
NFI	0.579±0.067	0.875±0.033	0.912±0.025
Symmetry	0.549±0.066	0.562±0.049	0.579±0.046
Superior ratio	0.550±0.066	0.684±0.043	0.710±0.040
Inferior ratio	0.525±0.066	0.728±0.041	0.749±0.038
Superior/nasal	0.600±0.061	0.704±0.042	0.775±0.036
Maximum modulation	0.572±0.062	0.767±0.038	0.810±0.033
Superior maximum	0.592±0.061	0.787±0.036	0.848±0.030
Inferior maximum	0.626±0.060	0.849±0.031	0.889±0.025
Ellipse modulation	0.595±0.061	0.732±0.041	0.715±0.040
Normalized superior area	0.545±0.064	0.816±0.034	0.855±0.029
Normalized inferior area	0.650±0.058	0.865±0.029	0.899±0.024

Table 6 Comparison of RNFL thickness measurements by OCT in control, OHT, GS, and EG eyes

Parameter (μm, mean ± SD)	Control	OHT	GS	EG	*P* value
Average	123.8±10.9	115.8±12.1	101.7±13.3	95.7±15.5	<0.001*
Quadrants					
Superior	147.4±18.1	139.2±19.2	123.9±19.7	117.0±21.1	<0.001†
Temporal	103.1±19.8	94.3±17.7	82.5±17.2	85.4±18.3	<0.001†
Inferior	146.0±17.8	138.3±17.7	118.2±21.4	101.5±23.8	<0.001†‡§¶
Nasal	95.5±18.0	89.0±26.1	79.9±18.5	76.1±20.6	<0.001†
Clock hours					
12	150.4±25.9	137.5±25.0	126.2±25.8	118.3±25.2	<0.001†
11 (superior temporally)	155.9±23.0	143.9±23.7	128.3±22.9	123.0±31.8	<0.001†‡
10	114.9±20.9	110.1±19.0	94.5±18.9	94.7±23.9	<0.001†§
9 (temporal)	87.5±17.4	83.9±17.2	70.5±19.0	78.1±19.2	<0.001†
8	105.3±23.9	97.2±18.6	85.5±22.4	84.4±24.2	<0.001†
7 (inferior temporally)	160.6±24.2	153.6±17.4	129.0±27.6	99.2±34.6	<0.001†‡§¶
6	153.8±22.7	142.7±28.8	123.4±28.5	103.7±31.0	<0.001†‡§¶
5	125.7±22.2	116.3±18.9	102.0±20.7	99.5±23.2	<0.001†‡§
4	95.0±21.0	89.2±34.3	78.2±19.3	74.7±26.3	<0.001‡§
3 (nasal)	832.9±18.3	74.0±30.2	68.1±22.6	63.3±21.8	<0.001†
2	109.1±22.1	98.6±27.6	93.7±24.7	91.0±26.1	<0.001†
1	135.1±22.5	134.4±25.1	117.2±29.1	112.0±28.1	<0.001†‡§
Sector classification					
Superior 120	138.4±15.4	130.3±15.8	116.5±17.0	111.7±19.9	<0.001†‡§
Temporal 50	96.6±16.9	91.9±15.6	78.3±17.5	82.7±18.2	<0.001†‡
Inferior 120	135.4±13.9	126.9±14.3	109.4±17.1	95.9±20.6	<0.001†‡§¶
Nasal 70	93.9±16.5	85.5±27.4	78.3±18.4	74.5±20.0	<0.001†

*Each group is significantly different from other groups
†Control is significantly different from OHT and GS
‡OHT is significantly different from EG
§OHT is significantly different from GS and EG
¶GS is significantly different from EG

Table 7 Area under the curve for OCT measurements

Parameter (mean ± SD)	OHT	GS	EG
Average	0.688±0.055	0.869±0.026	0.919±0.021
Quadrants			
Superior	0.614±0.061	0.799±0.035	0.857±0.029
Temporal	0.588±0.063	0.733±0.038	0.740±0.038
Inferior	0.649±0.059	0.865±0.029	0.924±0.021
Nasal	0.582±0.063	0.710±0.042	0.722±0.036
Clock hours			
12	0.641±0.059	0.747±0.039	0.803±0.034
11(superior temporally	0.643±0.059	0.792±0.035	0.789±0.035
10	0.579±0.063	0.757±0.038	0.723±0.039
9 (temporal)	0.579±0.063	0.621±0.039	0.634±0.043
8	0.577±0.063	0.719±0.041	0.735±0.038
7 (inferior temporally	0.632±0.060	0.828±0.034	0.923±0.020
6	0.622±0.061	0.817±0.034	0.894±0.024
5	0.639±0.059	0.782±0.037	0.781±0.035
4	0.537±0.065	0.719±0.041	0.735±0.038
3 (nasal)	0.614±0.061	0.697±0.042	0.755±0.036
2	0.614±0.061	0.661±0.045	0.692±0.040
1	0.509±0.066	0.671±0.044	0.734±0.039
Sector classifications			
Superior-120	0.648±0.059	0.820±0.034	0.849±0.030
Temporal-50	0.594±0.062	0.763±0.038	0.710±0.040
Inferior-120	0.696±0.055	0.867±0.029	0.932±0.020
Nasa-70	0.611±0.061	0.720±0.041	0.773±0.036

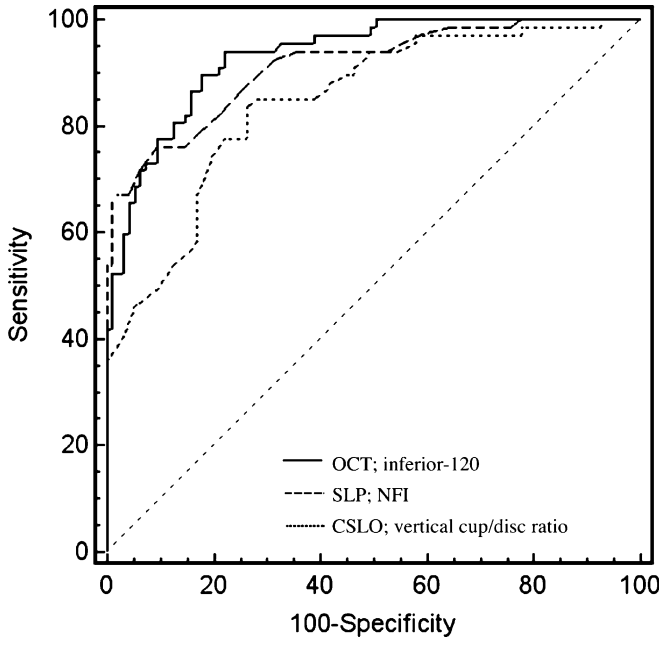

Fig. 1 Receiver operating characteristic (ROC) curves of confocal scanning laser ophthalmoscopy (*CSLO*), scanning laser polarimetry (*SLP*), and optical coherence tomography (*OCT*) parameters with the greatest area under the curve (AUC) for discriminating early glaucomatous (EG) from normal eyes. *NFI* nerve fiber indicator

tween control and OHT. Parameters between EG and GS that did show a significant difference were the nerve fiber indicator (NFI) and the inferior average. AUCs from SLP is demonstrated in Table 5. The SLP parameters with greatest AUC in EG, GS and OHT were NFI, NFI, and normalized inferior area, respectively.

Table 6 summarizes RNFL thickness measurements by OCT. The RNFL thickness in all parameters of EG and GS was significantly lower compared with control eyes. Except for the average RNFL thickness, there were no parameters showing significant differences between normal eyes and OHT. Parameters with a significant difference between EG and GS were related to the inferior area. AUCs from OCT are shown in Table 7. The RNFL thickness by OCT with the greatest AUC in EG, GS and OHT were inferior 120, average, and inferior 120 respectively.

Comparison of the discriminating ability of CSLO, SLP, and OCT

Figure 1 shows the ROC curves with the greatest AUC for each instrument in EG eyes. The CSLO parameter vertical cup/disc ratio had a significantly lower AUC than the OCT inferior 120 (P=0.023). Regarding AUCs distinguishing GS from normal eyes, CSLO (global cup shape measure)

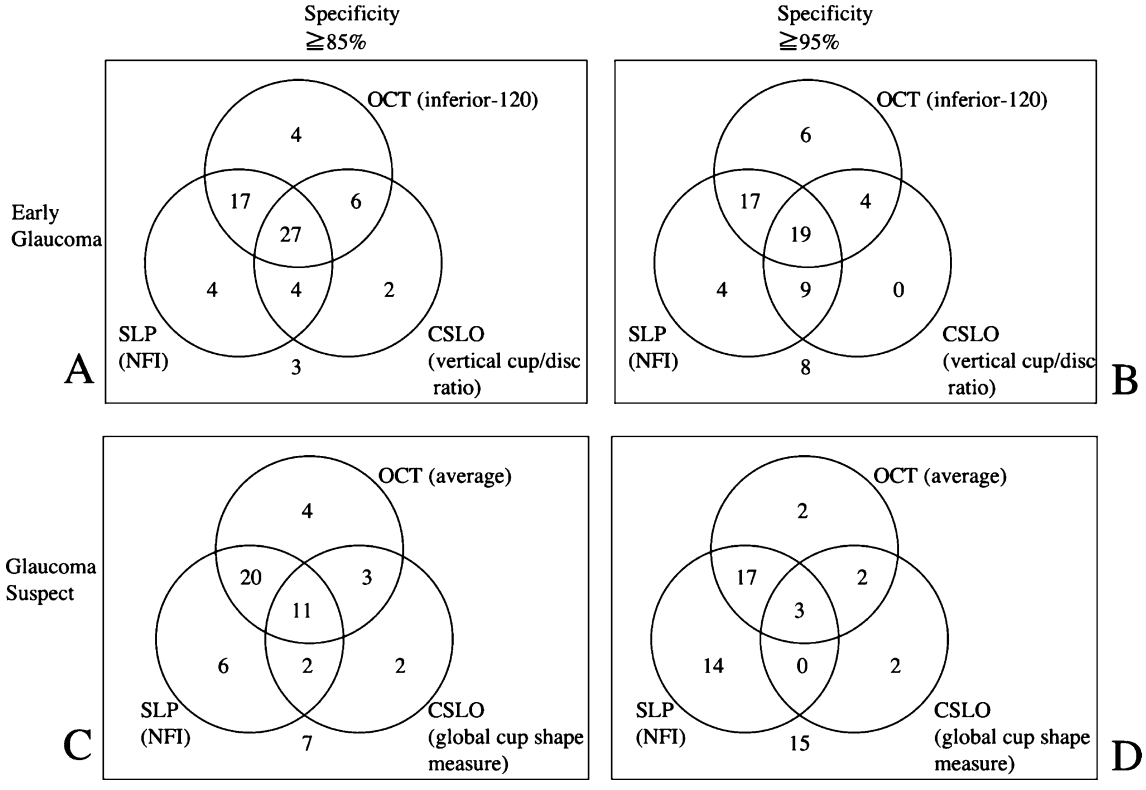

Fig. 2 Venn diagrams showing the number of eyes discriminated from normal as **a**,**b** early glaucomatous or **c**,**d** glaucoma suspect by parameters with the greatest AUC for each instrument at a fixed specificity of at least **a**,**c** 85% or **b**,**d** 95%

Table 8 Parameters with the greatest AUC per sector demonstrating the ability to distinguish early glaucoma from normal eyes

	AUC	*P* value*			Sensitivity/specificity (%)		
		CSLO vs. SLP	CSLO vs. OCT	SLP vs. OCT	Best value	Specificity ≧95%	Specificity ≧85%
Global sector		0.097	0.052	0.779			
CSLO: vertical cup/disc ratio	0.845				84/72	36/96	54/87
SLP: NFI	0.912				76/91	67/96	79/85
OCT: average	0.919				78/94	66/96	84/85
Superior sector		0.148	0.277	0.668			
CSLO: cup/disc area ratio	0.812				71/78	36/96	61/85
SLP: superior average	0.869				69/92	57/96	70/85
OCT: superior quadrant	0.857				75/81	49/95	67/85
Inferior sector		0.122	0.017†	0.240			
CSLO: cup/disc area ratio	0.842				81/75	45/96	66/85
SLP: inferior average	0.905				87/86	72/96	87/85
OCT: inferior 120	0.932				81/87	66/96	82/85

*Comparison using Hanley and McNeil's method
†Significant difference

had a significantly lower AUC than SLP (NFI, *P*=0.005) and OCT (average RNFL thickness, *P*=0.005). In contrast, there were no significant differences in the greatest AUC among instruments in OHT (CSLO; temporal cup volume, SLP; normalized inferior area, OCT; inferior 120).

Sensitivity of EG eyes was 95.5% (64 out of 67) with the greatest AUC parameter from at least one instrument at a specificity of 85% (Fig. 2a). At a specificity of 95%, 88.1% (59 out of 67) of EG eyes could be detected by SLP or OCT. In other words, 11.9% (8 out of 67) of EG eyes could not be discriminated by any instruments alone or combinations of these (Fig. 2b). On the other hand, 72.7% (40 out of 55) and 87.3% (48 out of 55) of GS eyes could be distinguished from normal eyes by the greatest AUC parameter by at least one instrument at a specificity of 95% and 85% respectively (Fig. 2c,d).

Sector analysis

Tables 8 and 9 show the measurements with the greatest AUC in the global, superior, and inferior sectors in EG and GS eyes respectively. Sensitivity and specificity were also demonstrated by obtaining the highest sensitivity values

Table 9 Parameters with the greatest AUC per sector demonstrating the ability to distinguish glaucoma-suspect from normal eyes

	AUC	*P* value*			Sensitivity/specificity(%)		
		CSLO vs. SLP	CSLO vs. OCT	SLP vs. OCT	Best value	Specificity ≧95%	Specificity ≧85%
Global sector		0.005†	0.005†	0.885			
CSLO: cup shape measure	0.722				62/78	13/96	33/86
SLP: NFI	0.875				62/94	55/96	64/85
OCT: average	0.869				86/78	44/96	67/85
Superior sector		0.078	0.081	0.906			
CSLO: cup/disc area ratio	0.718				60/79	27/96	46/85
SLP: normal superior ratio	0.816				71/79	40/96	62/85
OCT: superior 120	0.820				84/66	35/96	58/85
Inferior sector		0.002†	0.002†	0.939			
CSLO: cup/disc area ratio	0.701				81/75	45/96	66/85
SLP: normal inferior ratio	0.865				78/84	38/96	73/85
OCT: inferior 120	0.867				80/84	51/96	71/85

*Comparison using Hanley and McNeil's method
†Significant difference

with a target specificity set at 95% and 85% or at the highest accuracy (minimal false-negative and false-positive results). In EG, the CSLO parameter had a significantly lower AUC than the OCT measurements, but only in the inferior sector (P=0.017). In GS, the SLP parameter and the OCT measurements had a significantly higher AUC than the CSLO in the global area and inferior sector (P<0.01).

Discussion

The analyses of data in the current study could be divided into two aspects, the first being comparison of parameter values measured by the CLSO, SLP, and OCT among normals, OHT, GS, and EG, and the second consisting of a comparison of the ability of each instrument to detect early-stage glaucomatous damage.

Our result demonstrated that most parameters in each instrument could be used to distinguish normal eyes from GS or EG eyes. However, there were no significant differences in most parameters between normal eyes and OHT eyes, which were in agreement with previous reports [10, 14, 16, 28]. On the other hand, there was a difference in average RNFL thickness measured by OCT between normal eyes and OHT eyes, which suggests that marginal RNFL thickness reduction may precede the glaucomatous changes of the optic disc configuration. However, AUCs in all parameters were low and thus these instruments were not optimal for distinguishing OHT from a normal eye. A possible reason for this is that OHT in this study was defined simply based on IOP of over 21 mmHg, which may have been affected by the central corneal thickness. Although we unfortunately could not measure the central corneal thickness in normal controls, the central corneal thickness in eyes with OHT was 556.5±24.4 (mean ± standard deviation) ranging from 512 to 594 μm, which was relatively thin compared with previous reports. Thus, IOP of eyes with OHT measured in this study actually seemed high. Another reason may be the small OHT sample size in this study. Finally, the versions of the instruments used were old. The latest versions of OCT3 may evaluate not only RNFL thickness, but also the optic nerve head configuration. The update of the instruments may improve their ability to detect subtle anatomical changes in OHT.

There are a few reports on comparisons among normal, EG, and GS eyes using one or two instruments [4, 14, 17, 28]. The relatively high AUCs for the three instruments tested in the present study to discriminate glaucomatous changes were in good agreement with these previous reports.

Regarding the comparison of the ability to discriminate glaucoma among the three instruments, only three reports have been published to our knowledge. Two reports described that the difference in the greatest AUC was not significant among the HRT-1, GDx, and OCT-1 with version A4X1 software [5, 29]. Recently, Medeiros et al. [15] compared the ability of HRT-II, GDx-VCC (software version 5.0.1), and STRARUS-OCT to diagnose glaucomatous optic neuropathy. According to them, AUCs for the best parameters from GDx-VCC (NFI, AUC=0.91) and STRATUS-OCT (inferior thickness, AUC=0.92) were relatively higher than that from HRT-II (Bathija function, AUC=0.86). Our results were similar to Medeiros' report, despite using the older version of OCT and HRT. On the other hand, the present study showed that the greatest CSLO parameter was significantly lower than the greatest AUC parameters from OCT in EG and SLP in both EG and GS eyes. One possible reason for this may be due to the fact that the optic discs in the Japanese were more frequently myopic in shape and distorted than those in Caucasians [25, 27]. Also, the anatomical distortions of the disc, such as individual variation and racial difference, may affect the reference plane setting and thus lead to the decreased AUC in HRT assessment of the disc [8].

When comparing SLP and OCT RNFL thickness measurements, it is important to consider the measurement distance from the optic disc [24] because RNFL thickness becomes thinner along the distance from the optic disc [20]. The standard set for conventional SLP measurements was an area 1.75 times the disc diameter, which was different from the measurement circle of OCT. In addition, it should also be noted that targets of measurements by SLP and OCT are different. OCT analyzes a retinal section from the inner retinal membrane to the posterior boundary, which is automatically calculated. Hence, RNFL thickness by OCT presumably includes not only ganglion cell axons, but also Müller cell processes and astrocytes [18, 23]. In contrast, SLP measures the RNFL thickness based on analysis of retardations developed by only retinal nerve fibers.

Figure 2 showed that when using parameters with the greatest AUC the three instruments could complementarily detect glaucomatous damage of individuals within the EG and GS group. The instruments in this study can assess different aspects of the optic disc and RNFL and are therefore likely to complement each other, as long as the measurements are reliable and reproducible.

In conclusion, CSLO (HRT version 3.04), SLP (GDx-VCC: version 5.3.2), and OCT (OCT-1: version A6X1) had the ability to identify early glaucomatous eyes. These SLP and OCT versions had similar performance and were superior to CSLO for detecting early glaucomatous damage. Complementary examinations of these imaging instruments could provide supplementary and valuable information for the diagnosis of early-stage glaucoma.

References

1. Altman DG (1991) Practical statistics for medical research. Chapman and Hall, New York, pp 397–425
2. Caprioli J, Park HJ, Ugurlu S, Hoffman D (1998) Slope of the peripapillary nerve fiber layer surface in glaucoma. Invest Ophthalmol Vis Sci 39:2321–2328
3. Cioffi GA, Robin AL, Eastman RD et al (1993) Confocal laser scanning ophthalmoscope. Reproducibility of optic nerve head topographic measurements with the confocal laser scanning ophthalmoscope. Ophthalmology 100:57–62
4. Colen TP, Tang NE, Mulder PG, Lemij HG (2004) Sensitivity and specificity of new GDx parameters. J Glaucoma 13:28–33
5. Greaney MJ, Hoffman DC, Garway-Heath DF, Nakla M, Coleman AL, Caprioli J (2002) Comparison of optic nerve imaging methods to distinguish normal eyes from those with glaucoma. Invest Ophthalmol Vis Sci 43:140–145
6. Hanley JA, McNeil BJ (1983) A method of comparing the areas under receiver operating characteristic curves derived from the same cases. Radiology 148:839–843
7. Hee MR, Izatt JA, Swanson EA et al (1995) Optical coherence tomography of the human retina. Arch Ophthalmol 113:325–332
8. Hermann MM, Theofylaktopoulos I, Bangard N et al (2004) Optic nerve head morphometry in healthy adults using confocal laser scanning tomography. Br J Ophthalmol 88:761–765
9. Hoh ST, Ishikawa H, Greenfield DS, Liebmann JM, Chew SJ, Ritch R (1998) Peripapillary nerve fiber layer thickness measurement reproducibility using scanning laser polarimetry. J Glaucoma 7:12–15
10. Iester M, Broadway DC, Mikelberg FS, Drance SM (1997) A comparison of healthy, ocular hypertensive, and glaucomatous optic disc topographic parameters. J Glaucoma 6:363–370
11. Iester M, Mikelberg FS, Drance SM (1997) The effect of optic disc size on diagnostic precision with the Heidelberg retina tomograph. Ophthalmology 104:545–548
12. Jonas JB, Schmidt AM, Muller-Bergh JA, Schlotzer-Schrehardt UM, Naumann GO (1992) Human optic nerve fiber count and optic disc size. Invest Ophthalmol Vis Sci 33:2012–2018
13. Kanamori A, Escano MF, Eno A et al (2003) Evaluation of the effect of aging on retinal nerve fiber layer thickness measured by optical coherence tomography. Ophthalmologica 217:273–278
14. Kanamori A, Nakamura M, Escano MF, Seya R, Maeda H, Negi A (2003) Evaluation of the glaucomatous damage on retinal nerve fiber layer thickness measured by optical coherence tomography. Am J Ophthalmol 135:513–520
15. Medeiros FA, Zangwill LM, Bowd C, Weinreb RN (2004) Comparison of the GDx VCC scanning laser polarimeter, HRT II confocal scanning laser ophthalmoscope, and stratus OCT optical coherence tomograph for the detection of glaucoma. Arch Ophthalmol 122:827–837
16. Mistlberger A, Liebmann JM, Greenfield DS et al (2002) Assessment of optic disc anatomy and nerve fiber layer thickness in ocular hypertensive subjects with normal short-wavelength automated perimetry. Ophthalmology 109:1362–1366
17. Nouri-Mahdavi K, Hoffman D, Tannenbaum DP, Law SK, Caprioli J (2004) Identifying early glaucoma with optical coherence tomography. Am J Ophthalmol 137:228–235
18. Parisi V, Manni G, Centofanti M, Gandolfi SA, Olzi D, Bucci MG (2001) Correlation between optical coherence tomography, pattern electroretinogram, and visual evoked potentials in open-angle glaucoma patients. Ophthalmology 108:905–912
19. Poinoosawmy D, Fontana L, Wu JX et al (1997) Variation of nerve fiber layer thickness measurements with age and ethnicity by scanning laser polarimetry. Br J Ophthalmol 81:350–354
20. Quigley HA, Addicks EM (1982) Quantitative studies of retinal nerve fiber layer defects. Arch Ophthalmol 100:807–814
21. Quigley HA, Dunkelberger GR, Green WR (1989) Retinal ganglion cell atrophy correlated with automated perimetry in human eyes with glaucoma. Am J Ophthalmol 107:453–464
22. Quigley HA, Brown AE, Morrison JD, Drance SM (1990) The size and shape of the optic disc in normal human eyes. Arch Ophthalmol 108:51–57
23. Radius RL, Anderson DR (1979) The histology of retinal nerve fiber layer bundles and bundle defects. Arch Ophthalmol 97:948–950
24. Schuman JS, Pedut-Kloizman T, Hertzmark E et al (1996) Reproducibility of nerve fiber layer thickness measurements using optical coherence tomography. Ophthalmology 103:1889–1898
25. Shimizu N, Nomura H, Ando F et al (2003) Refractive errors and factors associated with myopia in an adult Japanese population. Jpn J Ophthalmol 47:6–12
26. Sommer A, Miller NR, Pollack I, Maumenee AE, George T (1997) The nerve fiber layer in the diagnosis of glaucoma. Arch Ophthalmol 95:2149–2156
27. Yamazaki Y, Yoshikawa K, Kunimatsu S et al (1999) Influence of myopic disc shape on the diagnostic precision of the Heidelberg Retina Tomograph. Jpn J Ophthalmol 43:392–397
28. Wollstein G, Garway-Heath DF, Fontana L, Hitchings RA (2000) Identifying early glaucomatous changes. Comparison between expert clinical assessment of optic disc photographs and confocal scanning ophthalmoscopy. Ophthalmology 107:2272–2277
29. Zangwill LM, Bowd C, Berry CC et al (2001) Discriminating between normal and glaucomatous eyes using the Heidelberg Retina Tomograph, GDx Nerve Fiber Analyzer, and Optical Coherence Tomograph. Arch Ophthalmol 119:985–993
30. Zeyen TG, Caprioli J (1993) Progression of disc and field damage in early glaucoma. Arch Ophthalmol 111:62–65
31. Zhou Q, Weinreb RN (2002) Individualized compensation of anterior segment birefringence during scanning laser polarimetry. Invest Ophthalmol Vis Sci 43:2221–2228